The American Journal of Pathology, Vol. 175, No. 4, October 2009
Copyright © American Society for Investigative Pathology
DOI: 10.2353/ajpath.2009.090462

Neurobiology

Overexpression of Wild-Type Murine Tau Results in Progressive Tauopathy and Neurodegeneration

Stephanie J. Adams, Richard J.P. Crook, Michael DeTure, Suzanne J. Randle, Amy E. Innes, Xin Z. Yu, Wen-Lang Lin, Brittany N. Dugger, Melinda McBride, Mike Hutton, Dennis W. Dickson, and Eileen McGowan

From the Department of Neuroscience, Mayo Clinic College of Medicine, Jacksonville, Florida

Here, we describe the generation and characterization of a novel tau transgenic mouse model (mTau) that overexpresses wild-type murine tau protein by twofold compared with endogenous levels. Transgenic tau expression was driven by a BAC transgene containing the entire wild-type mouse tau locus, including the endogenous promoter and the regulatory elements associated with the tau gene. The mTau model therefore differs from other tau models in that regulation of the genomic mouse transgene mimics that of the endogenous gene, including normal exon splicing regulation. Biochemical data from the mTau mice demonstrated that modest elevation of mouse tau leads to tau hyperphosphorylation at multiple pathologically relevant epitopes and accumulation of sarkosyl-insoluble tau. The mTau mice show a progressive increase in hyperphosphorylated tau pathology with age up to 15 to 18 months, which is accompanied by gliosis and vacuolization. In contrast, older mice show a decrease in tau pathology levels, which may represent hippocampal neuronal loss occurring in this wild-type model. Collectively, these results describe a novel model of tauopathy that develops pathological changes reminiscent of early stage Alzheimer's disease and other related neurodegenerative diseases, achieved without overexpression of a mutant human tau transgene. This model will provide an important tool for understanding the early events leading to the development of tau pathology and a model for analysis of potential therapeutic targets for sporadic tauopathies. ***(Am J Pathol 2009, 175:1598–1609; DOI: 10.2353/ajpath.2009.090462)***

Abnormal accumulation of the microtubule-associated protein tau, in the form of neurofibrillary tangles (NFTs), is the defining pathological feature of neurodegenerative diseases termed tauopathies. Six major tau protein isoforms are generated in adult human brain by alternative splicing of the tau (*MAPT*) gene,[1,2] and studies of mutations within this gene have provided insight into potential mechanisms for the pathological aggregation of tau proteins.[3,4] With use of a single isoform of mutant human tau, transgenic mice have been generated (reviewed in [5]) that recapitulate many features of human tauopathy; however, most tauopathies are not associated with specific *MAPT* mutations. Because normal and mutant tau proteins appear to have functional differences,[6–8] the mechanism of tau pathology development, neuronal loss, and interactions with other proteins may also differ between sporadic tauopathies and cases linked to specific mutations. Previous attempts to create a wild-type tauopathy model through overexpression of a *single* wild-type human tau isoform have generally led to minimal pathological changes. Although these models have been useful in studying early aspects of tauopathy, they do not mimic normal gene regulation or tau isoform profiles in the brain. Development of a mouse model overexpressing the entire human tau transgene (8c mice) was expected to overcome this limitation. However, these mice failed to elicit notable tau pathology, but did result in a significant shift in exon 10 splicing compared with that in human brain. The explanation for this shift toward >90% expression of the three-repeat (3R) isoforms[9] and its significance in the absence of tau pathology remains uncertain.

Supported by a National Institute on Aging (NIA), NIH P01 Grant AG017216 (to D.W.D. and M.H.), a National Research Service Award postdoctoral fellowship AG027638 from NIA, NIH (to S.J.A.), and a Robert and Clarice Smith Fellowship (to S.J.A.).

Accepted for publication June 26, 2009.

S.J.A., R.J.P.C., M.H., E.M., and Mayo Clinic have an intellectual property and financial interests associated with the mTau mice and have received annual royalties from the licensing of the technology of less than the federal threshold for significant financial interest.

Supplemental material for this article can be found on *http://ajp.amjpathol.org*.

Address reprint requests to Stephanie J. Adams, Ph.D., Mayo Clinic College of Medicine, 4500 San Pablo Road, Jacksonville, FL 32224. E-mail: adams.stephanie@mayo.edu.

Interestingly, removal of the endogenous mouse tau gene (Htau mice) failed to return the splicing ratio to normal but did induce development of progressive tauopathy and neuronal loss.[10] Because the primary difference between the 8c and Htau lines is the presence of endogenous mouse tau, this finding suggested that murine tau may actually counter the aggregation of human tau in mouse models, which might explain the difficulty of inducing mature NFTs in the other wild-type human tau transgenic mice that also express endogenous mouse tau proteins. Mouse and human tau proteins are homologous (92%) over regions encoded by exons 2 to the C terminus but differ significantly (57%) within the amino terminus and in their isoform expression, with adult rodents almost exclusively expressing four-repeat (4R) tau[11] compared with the equivalent ratio of 3R to 4R found in adult humans.[7] Although *in vitro* studies have consistently shown no difference in human and mouse tau aggregation,[12–14] examples of other amyloidogenic peptides capable of aggregation individually, but showing a reduced rate of aggregation when combined in the same reaction do exist.[15,16] In addition, once aggregation has been initiated by mutant human tau overexpression, mouse tau is capable of aggregation and tangle formation *in vivo*.[17] We now describe a transgenic mouse model that develops age-related tau pathology and neurodegeneration, despite only moderate overexpression (<2 fold) of endogenous mouse tau from a genomic transgene, subject to normal gene regulation and exon 10 splicing ratios.

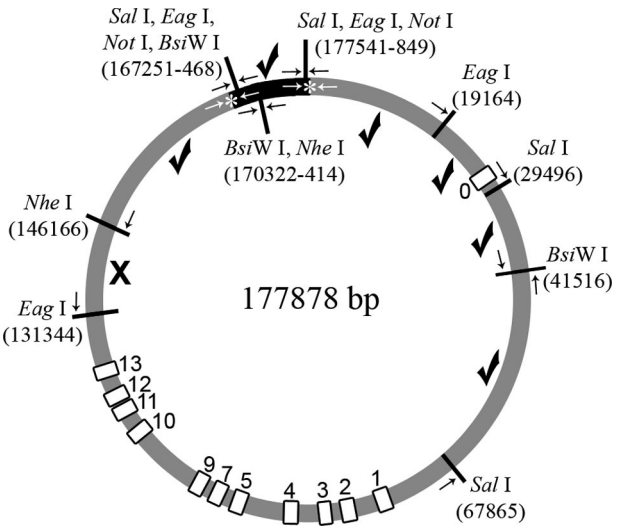

Figure 1. Diagram of BAC clone vector containing genomic mouse tau and iPCR experimental design. Created using Vector NTI software, the diagram shows the genomic region of the BAC (gray), the pTAR vector (black), and the locations of mouse tau exons (numbered white boxes), genotyping primers (**white arrows**) to genomic/vector boundaries (**asterisk**), and restriction enzyme and primer sites (**black arrows**) for iPCR, with one primer for each fragment located in the vector. Because inference is drawn from PCRs failing to amplify, BAC DNA was used as a positive control and wild-type mouse DNA was used as a negative control for PCR amplification. All products were sequenced to verify that the amplicons were the specified target product. Using this technique, we determined that the BAC clone linearized somewhere within a 15-kb region starting 7.5 kb downstream of tau (X between EagI and NheI sites) in 12 of the 13 original founders (data not shown).

Materials and Methods

BAC Preparation and Characterization

Genomic-free BAC DNA was isolated using a Qiagen Large-Construct Kit (Qiagen, Valencia, CA). Before its use as a transgene, we confirmed that the 177-kb BAC clone (RP24-271J17, BACPAC Resource Center; Oakland, CA) was intact and contained the mouse tau locus in its entirety through restriction enzyme mapping using XhoI and XmaI and pulsed field gel electrophoresis, which showed a banding pattern corresponding to the expected size of fragments based on Vector NTI software analysis. Smaller fragments (~5 kb to 79 bp) were resolved using conventional electrophoresis. Purified BAC DNA was further characterized by standard PCR to test for the presence of each exon, as well as other sites throughout the BAC clone, including the vector/genomic boundaries. Sequences generated from each of the genomic amplicons yielded no variants from the reference sequence (National Center for Biotechnology Information Build 33.1 NT_039521).

Generation of mTau Mice

Circularized BAC DNA (2.5 ng/μl) was injected into fertilized oocytes from FVB/N1 congenic mice to yield potential founders. Transgenic founders were identified by standard PCR from tail-clip digestions using a multiplex of primers designed (FastPCR freeware) against the two genomic/vector boundaries of the BAC (Figure 1, white arrows) to distinguish the transgene from the endogenous copy and β-actin as a positive control. Primers (V3F 5′-TCAAGGGCATCGGTCGAGCTTG-3′, G5R 5′-AGTGGCCTTTGTGGGGTACATC-3′, G3F 5′-TTAAAGGTGTGCGCCAGTG-3′, V5R 5′-CGATCTGCCGTTTCGATCCTCC-3′, ActBF 5′-GGCTACAGCTTCACCACCACAG-3′, and ActBR 5′-CAATAGTGATGACCTGGCCGTC-3′) were used in a multiplex reaction with an annealing temperature of 58°C. Because founder animals were generated from microinjections of circular DNA, which undergoes random linearization during incorporation into the genome, we confirmed that the transgenic mouse tau gene remained intact *in vivo*. Given that verification of the *in vivo* integrity of the transgene by Southern blotting would have been confounded by the presence of the endogenous copy of the mouse tau gene, we used inverse PCR (iPCR) to distinguish transgenic and endogenous tau. iPCR primers were designed in conjunction with specific restriction sites to amplify products of different sizes in the mouse tau BAC transgene versus the endogenous mouse tau region, thereby allowing us to specifically determine whether large regions of the transgene were intact *in vivo*. Primers were designed to be within the same restriction enzyme fragment, with one primer located within the vector sequence, as with the genotyping PCR assay, so as not to amplify the endogenous copy of the gene. Before digestion, the iPCR primers are designed to be in the wrong orientation to produce a product; however, after digestion and self-religation, the iPCR primers then "face" each other and will amplify the

region between them. Although intermolecular religation is possible, intramolecular or self-religation is favored at the low DNA concentrations used in these reactions. If the point of linearization of the BAC clone is between a pair of iPCR primers, those primers will fail to amplify because they will sit down on different religated fragments. Conversely, it can be inferred that a particular region of the transgene is intact if a given set of iPCR primers produce the expected amplicon. The BAC clone was used as a positive control for the success of iPCR reactions, and all products were sequenced to verify that the amplicons were the target product.

Mice were maintained on an FVB/N background (Harlan Laboratories, Indianapolis, IN) and housed in a barrier facility. All mice were humanely sacrificed by cervical dislocation at various time points, and brains were quickly removed for dissection. The left cerebral hemisphere was immediately fixed in 10% formalin, and the other hemisphere was frozen on dry ice for subsequent biochemical analysis.

Survival Curves

Genotyping of pups was performed after weaning at 21 days of age, and, therefore, reliable estimation of transgenic mice survival is limited to their postweaning age. Statistical analysis of survival was assessed by the Kaplan-Meier method with survival curves compared using pairwise (Holm-Sidak) multiple comparison procedures (GraphPad Software Inc., San Diego, CA).

Quantitative Real-Time RT-PCR

Total RNA was isolated from the right brain hemispheres of transgenic (Tg) mTau and nontransgenic (NTg) mice of each sex (three mice per group) harvested at 3 months of age using an RNeasy mini prep kit (Qiagen). Transgene expression levels were determined by real-time PCR measuring mRNA expression of mouse tau relative to endogenous β-actin using predeveloped TaqMan assays (assay Mm00521988_m1; Applied Biosystems, Foster City, CA) and an ABI 7900 instrument. Experimental wells containing 10-μl PCRs, including 100 ng of total RNA from each sample, were run in quadruplicate in 384-well plates. Expression results were calculated relative to β-actin expression, normalized to the lowest expressing littermate and averaged for Tg and NTg mice.

In Situ *Hybridization*

In situ hybridization was performed to determine the genomic mouse tau transgene expression profile. Frozen 3-month-old mTau mouse brains were sagittally sectioned at a thickness of 15 μm. Oligomers to tau exon 11 were end-labeled with α-[^{35}S]dATP. Slides were hybridized overnight at 37°C with labeled oligonucleotide in buffer containing 4× standard saline citrate, 1× Denhardt's solution, 50% w/v deionized formamide, 10% w/v dextran sulfate, 200 mg/μl herring sperm DNA, and 0.03% β-mercaptoethanol. After hybridization, the sections were stringently washed (1× standard saline citrate at 50°C), dehydrated, and exposed to β-max Hyperfilm (Amersham Biosciences, Piscataway, NJ) for 7 to 10 days. Control slides were hybridized in the presence of a 50-fold molar excess of unlabeled oligonucleotide.

RT-PCR Analysis of Splice Isoforms

Total RNA isolated from hemibrains of Tg and NTg mice of each sex (five mice per group) at 6 weeks was isolated as described above and analyzed by semi-quantitative RT-PCR for differences in splice isoform ratios. Mouse-specific primers designed to span either the N-terminal region (across exons 1 and 5) or to span the microtubule binding domain region (across exons 9 and 11) were used as described previously.[9] Htau mice, overexpressing genomic human tau on a mouse tau knockout background, were used as a control.[10] Primers that spanned alternatively spliced exon 10 would amplify tau splice isoforms encoding either 3R or 4R tau, and others were used to examine splicing of exons 2 and 3 encoding 0N, 1N, or 2N tau. Mouse and human-specific tau RT-PCR products were analyzed by gel electrophoresis, and isoforms were identified based on their expected sizes.

Brain Extract Preparation for Biochemistry

Harvested brain tissue was homogenized in buffer containing 50 mmol/L Tris, pH 8.0, 274 mmol/L NaCl, 5 mmol/L KCl, 2 mmol/L EGTA, 2 mmol/L EDTA, 100 mmol/L phenylmethylsulfonyl fluoride, protease inhibitor cocktail (Sigma-Aldrich, St. Louis, MO), and phosphatase inhibitor cocktails I and II (Sigma-Aldrich). Homogenates were centrifuged at 150,000 × *g* for 15 minutes, and the supernatant was collected as a total fraction. Purification of sarkosyl-insoluble tau (P3 fraction) was performed as described previously.[18] The amount of starting material was adjusted for protein concentration to obtain comparable results. The supernatant was centrifuged at 150,000 × *g* for 15 minutes to separate proteins into soluble (S1, supernatant) and insoluble (pellet) fractions. The pellet was then re-extracted via homogenization in buffer B containing 10 mmol/L Tris HCl, pH 7.4, 0.8 M NaCl, 10% sucrose, 1 mmol/L EGTA, and 1 mmol/L phenylmethylsulfonyl fluoride, protease inhibitor cocktail (Sigma-Aldrich), and phosphatase inhibitor cocktails I and II (Sigma-Aldrich) and centrifuged again at 150,000 × *g* for 15 minutes. The pellet was discarded, and the buffer B supernatant was incubated with 1% sarkosyl at 37°C for 1 hour followed by another centrifugation at 150,000 × *g* for 30 minutes. The supernatant was collected as a salt-extractable (S2) fraction, and the pellet (solubilized in TE buffer: 10 mM Tris, pH 8.0, 1 mM EDTA) contained the sarkosyl-insoluble tau (P3) fraction. Typically, 600 μl of total extract was used to obtain 20 μl of P3 fraction.

Western Blotting

A total of 10 μg of proteins for the total and S1 fraction and 10 μl for the P3 fraction were mixed with equivalent

volume of 2× SDS sample buffer (Invitrogen, Carlsbad, CA) (62.5 mmol/L Tris-HCl, pH 6.8, 2% SDS, 25% glycerol, and 0.1% bromphenol blue) and 5% β-mercaptoethanol, boiled for 5 minutes, and loaded onto 10% polyacrylamide Tris-glycine gels (Invitrogen). The gels were resolved at 125 V for ~3 hours and then transferred onto a polyvinylidene difluoride membrane using a wet transfer system at 200 mA for 90 minutes. The membrane was blocked with either 5% milk or Odyssey blocking buffer (LI-COR Biosciences, Lincoln, NE) and incubated in primary antibody overnight at 4°C. The membrane was then washed three times for 10 minutes each with TBST (1% Triton X-100, 10 mmol/L Tris, and 140 mmol/L NaCl), incubated in secondary antibody (either horseradish peroxidase conjugated for standard Western blotting or fluorescein conjugated for Odyssey blots) for 1 hour at room temperature, washed three times for 10 minutes each with TBST, and once with Tris-buffered saline (TBS). Standard Western blots were then incubated with Western Lightning Chemiluminescence Reagent Plus (PerkinElmer Life and Analytical Sciences, Wellesley, MA) and exposed on BioMax Light film (Eastman Kodak, Rochester, NY). The films were scanned, and densitometric analysis was performed using ImageJ software.[19] Odyssey blots were scanned using a LI-COR scanner and densitometric analysis was performed using Odyssey software (LI-COR Biosciences, Lincoln, NE). The intensity of the protein band of interest was normalized against a loading control, glyceraldehyde-3-phosphate dehydrogenase.

Antibodies

Biochemical and immunohistochemical analysis was performed with a number of antibodies Tau 5 (mouse monoclonal total tau antibody (1:200; (Neomarkers, Freemont, CA)); CP13 phospho-tau S202 mouse monoclonal antibody and PHF1 phospho-tau S396/S404 mouse monoclonal antibody (1:1000; provided by Dr. P. Davies, Albert Einstein College of Medicine, Bronx, NY); AT8 phospho-tau S202/T205 mouse monoclonal antibody (1:100; Pierce, Rockford, IL); glyceraldehyde-3-phosphate dehydrogenase mouse monoclonal antibody (1:5000; Biodesign International, Kennebunkport, ME); glial fibrillary acidic protein (GFAP) rabbit polyclonal antibody (1:10,000; BioGenex, San Ramon, CA), MS06, polyclonal antibody specific to mouse tau (1:2000; provided by Dr. A. Takashima, RIKEN Brain Science Institute, Wako City, Japan), carbonic anhydrase II antibody (CAII, 1:10,000 in 5% normal goat serum; provided by Dr. M. S. Ghandour), shown to specifically label oligodendrocytes,[20] neuron-specific nuclear protein (NeuN) mouse monoclonal antibody (1:100; Chemicon International, Billerica, MA), and horseradish peroxidase-conjugated secondary antibodies (1:5000; Jackson ImmunoResearch Laboratories, West Grove, PA) or fluorescein-conjugated secondary antibodies (1:2000; Molecular BioProbes, Eugene, OR).

Immunohistochemistry

Immunohistochemistry was performed on brain tissue from Tg and NTg mice of each gender (five mice per group) at various ages (6 to 22 months). Coronal sections (5-μm paraffin embedded) were mounted on glass slides, deparaffinized, rehydrated in xylene and a graded series of alcohol, and subjected to antigen retrieval with steam in distilled H_2O for 30 minutes. Sections were incubated with 3% H_2O_2 to block endogenous peroxidase activity. Before staining with any mouse-specific antibodies, sections were treated with the MOM kit (Vector Laboratories, Burlingame, CA) to block nonspecific mouse on mouse binding for 1 hour at room temperature. The tissue sections, along with positive and negative controls, were processed in a batch for uniformity, using a Autostainer and Envision peroxidase methods (Dako North America, Carpenteria, CA) and developed with 3,3′-diaminobenzidine. The stained slides were lightly counterstained with hematoxylin, dehydrated, and coverslipped. CP13, AT8, and PHF1 were used to detect hyperphosphorylated tau, and Gallyas silver staining[21] was used to detect NFT formation. GFAP and CAII were used as astrocyte and oligodendrocyte markers, respectively. NeuN was used as a neuron-specific antibody. Burden analysis for tau and NeuN was determined using an Aperio slide scanner and ImageScope image analysis software (positive pixel count algorithm). Vacuole pathology was analyzed by scoring done blinded to genotype, age, and gender (scale: 0, none; 1, mild;, 2, intermediate; or 3, severe).

Fluorescent Immunohistochemistry and Colocalization Studies

Fluorescent immunohistochemistry and double labeling were performed with GFAP alone, GFAP and CP13, or CAII and CP13 antibodies. Sections were incubated in primary antibodies for 2 to 3 hours at room temperature, washed in 0.1 M PBS, incubated in biotinylated goat anti-rabbit and goat anti-mouse antibodies (1:1000) followed by fluorescein-conjugated streptavidin secondary antibodies (1;500) for 30 minutes each at room temperature, and washed in 0.1 M PBS. Autofluorescence was blocked by applying Sudan black (Sigma-Aldrich) for 5 minutes, and slides were washed and cover-slipped using Pro-Long antifade medium (Molecular BioProbes). Slides were examined using the Olympus Confocal microscope running Fluroview acquisition software. Images were collected using single excitation for each wavelength separately, and channels were subsequently merged.

Electron Microscopy

For electron microscopy, 18-month-old Tg and NTg mice were perfused with saline followed by 2.5% glutaraldehyde/2% paraformaldehyde/0.1 M cacodylate buffer. The hippocampus was removed, cut into 2-mm^3 pieces, postfixed in 1% osmium tetroxide and 1% uranyl acetate, dehydrated in a series of alcohol and propylene oxide, infiltrated, and embedded in Epon 812. Thin sections were stained with uranyl acetate and lead citrate before examination with a Philips 208S electron microscope (Philips, Hillsboro, OR).

Immunogold Negative Stain Electron Microscopy

Sarkosyl-insoluble samples were collected as described above except that the high-salt buffer B fractions containing 10% sucrose were clarified at 20,000 × *g* for 15 minutes before addition of 1% sarkosyl to the buffer B supernatant. After incubation at 37°C for 1 hour, these samples were split into two parts for P3 isolation for Western blotting or further sucrose gradient purification for electron microscopy. The sucrose fractionation was performed by layering 200 μl of the samples in high-salt buffer plus sarkosyl onto a gradient containing 1-ml steps of 30, 50, and 70% sucrose in TBS pH 7.4 as described previously.[22] After centrifugation at 160,000 × *g* for 16 hours, 400-μl samples were collected at the top of the column and at each interface. The sarkosyl-insoluble materials were diluted 1:20 in TE buffer and adsorbed on to carbon/Formvar-coated 400-mesh copper grids (EM Sciences) for 45 seconds. The grids were washed three times with filtered TBS, blocked for 30 minutes on a filtered TBS solution containing 0.5% bovine serum albumin, and then incubated for 1 hour with the primary antibody WKS44 antibody (provided by Dr. S-H. Yen, Mayo Clinic, Jacksonville, FL) that recognizes a nonphosphorylated tau epitope diluted 1:50 in blocking solution. Grids were then washed three times in blocking solution, and the grids were incubated for 1 hour in blocking solution containing 10-nm gold-conjugated anti-rabbit secondary antibody (1:20 dilution, Amersham Biosciences, Pittsburgh, PA). After grids were washed five times with TBS, they were then stained with 2% uranyl acetate for 45 seconds and examined with an EM 208S electron microscope (Phillips, Hillsboro, OR). Tau aggregates were predominantly found in the 30 to 50% sucrose interface, and electron micrographs were only collected on samples containing at least four gold particles.

Statistics

Statistical analysis was performed using SigmaPlot 11.0 (Systat Software, Inc., San Jose, CA). Data are expressed as mean ± SEM and analyzed using either *t*-test, analysis of variance, and/or Spearman rank-order correlation tests where appropriate, with $P < 0.05$ considered significant. Unless otherwise stated, 10 Tg and 10 NTg mice (5 mice per sex) were used per time point. Two-tailed unpaired *t*-tests were performed using Microsoft Excel where noted. All graphing was performed using GraphPad Prism software (GraphPad Software Inc., San Diego, CA).

Results

Generation of mTau Mice

We generated a novel transgenic mouse model overexpressing genomic wild-type mouse tau using a BAC-derived transgene (mTau model). Purified BAC DNA isolated from a BAC clone containing the mouse tau gene was subjected to restriction enzyme mapping to confirm that the mouse tau gene was intact and contained the mouse tau gene in its entirety before its use as a transgene. The BAC DNA showed a banding pattern corresponding to the expected size of fragments for an XhoI restriction enzyme digest based on Vector NTI software analysis (data not shown). Sequencing showed that the BAC DNA contained all 13 tau exons, as well as all of the XhoI sites with no variants from the reference sequence (National Center for Biotechnology Build 33.1 NT_039521) observed in any of the amplicons.

Circular BAC DNAs were injected into fertilized oocytes from FVB/N1 congenic mice; from these injections, 10 founder litters consisting of 110 pups were produced, and 13 founders were confirmed to be positive for the BAC mouse tau transgene. Because these founder animals were generated from microinjections of circular DNA, which undergoes random linearization during incorporation into the genome, it was necessary to confirm that the transgenic mouse tau gene remained intact *in vivo*. This was accomplished using iPCR techniques, which enabled us to distinguish between the transgenic and the endogenous copies of the mouse tau gene. For the mouse tau transgene to be functional it must be intact from the promoter, approximately 1 kb upstream of exon 0, through all 13 coding exons. Using Vector NTI software, we identified several restriction enzymes that cut within the vector and the genomic region of the 177-kb BAC clone. These enzymes were used to divide the BAC clone into as many regions as possible to identify the linearization point of the circular BAC DNA *in vivo* and confirm that the linearization did not occur within the tau gene itself (Figure 1). Using different iPCR primers/restriction enzymes combinations (see *Materials and Methods* and Figure 1 for details), we determined that the BAC clone linearized somewhere within a 15-kb region starting 7.5 kb downstream of the tau gene in 12 of the 13 original founders (data not shown), confirming that the transgenic tau gene was intact in these 12 founders.

Eleven of the original founders were mated to FVB/N congenic mice. Although multiple mTau founders were generated, approximately 40% (4 of 11) were either infertile or had offspring with significant perinatal mortality. All nonbreeding founders showed tau protein overexpression >1.9-fold above that of endogenous tau as determined by Western blot analysis (Figure 2A). In contrast, the breeding founders showed tau protein expression levels that were <1.8-fold above endogenous levels (see below). To provide an initial assessment of the impact of overexpressing mouse tau, the four nonbreeding founder mice were harvested between 6 and 8 months of age and examined neuropathologically. All of the nonbreeding founders had significant abnormal tau immunostaining, observed using the CP13 and AT8 antibodies, in both neuronal and glial cell populations. Granular hyperphosphorylated tau immunoreactivity in the cytoplasm and cell processes of neurons, consistent with pretangle pathology, was seen in the cortex and hippocampus (Figure 2, B–D; data not shown). Additional tau glial inclusion pathology in white matter (Figure 2E) was observed in small cells with morphology consistent with that of oligodendrocytes. The extent of the tau pathology in the nonbreeding founders varied within each mouse, re-

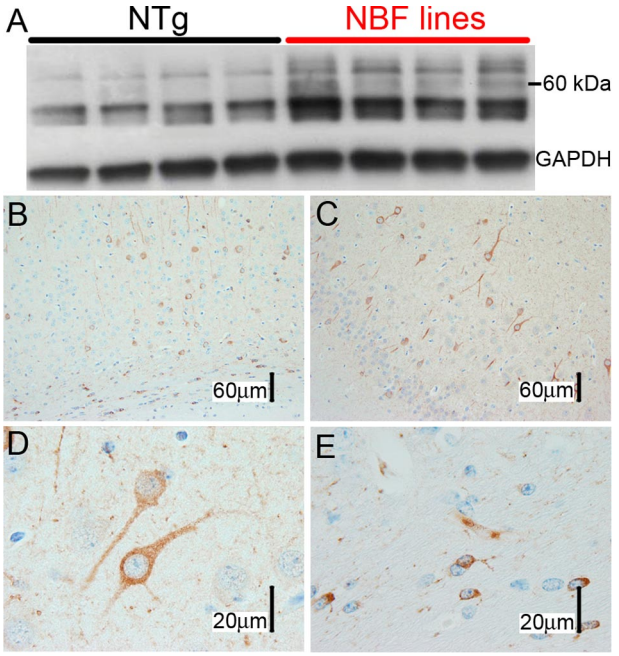

Figure 2. Non-breeding founders (NBFs). **A:** Protein expression levels. Immunoblot of NBFs, showing total soluble tau levels compared with NTg mice. Blots were probed with MS06 (mouse tau-specific antibody). NBFs expressed a range of trangenic protein levels up to 2.3-fold over endogenous tau levels based on densitometric analysis. Western results were in agreement with RT-PCR analysis. **B–E:** Pre-tangle pathology. NBF mice were harvested between 8 and 9 months of age. Immunohistochemistry shows hyperphosphorylated tau (CP13 immunoreactivity) in multiple forebrain areas including the motor cortex (**A**) and the piriform cortex (**B**). **C:** A higher magnification (×100) of **B** shows granular CP13 tau immunoreactivity in the cytoplasm and neuronal processes consistent with pretangle pathology. Abnormal tau pathology was also evident in oligodendocytes (**D**). All NBF mice had similar patterns of pretangle pathology in the brain.

flecting different transgene expression levels, although the qualitative pattern of the immunoreactivity was similar. These data demonstrated that wild-type mouse tau overexpression was able to cause pretangle formation in various brain regions and provided a strong rationale for continuing to develop the remaining mTau breeding lines.

Expression of Wild-Type Genomic Mouse in the mTau Mice

Genomic mouse transgenic tau expression in the fertile founder lines was determined using real time RT-PCR and ranged from 0 to 1.8-fold overexpression relative to the endogenous tau gene (data not shown). The highest expressing fertile founder lines (approximately 1.78-fold overexpression of tau relative to NTg as determined by both real-time PCR and Western analysis) were expanded and bred to homozygosity. *In situ* hybridization showed an expression pattern in these transgenic lines similar to the endogenous tau mRNA in nontransgenic littermates (Figure 3, A and B). Tau is ubiquitously expressed in the forebrain, mostly in neuronal cells. Optical density analysis of tau mRNA signals from the *in situ* hybridization (Figure 3B), as well as, tau protein levels determined by Western blot relative to NTg were consistent with the real-time PCR data, showing between approxi-

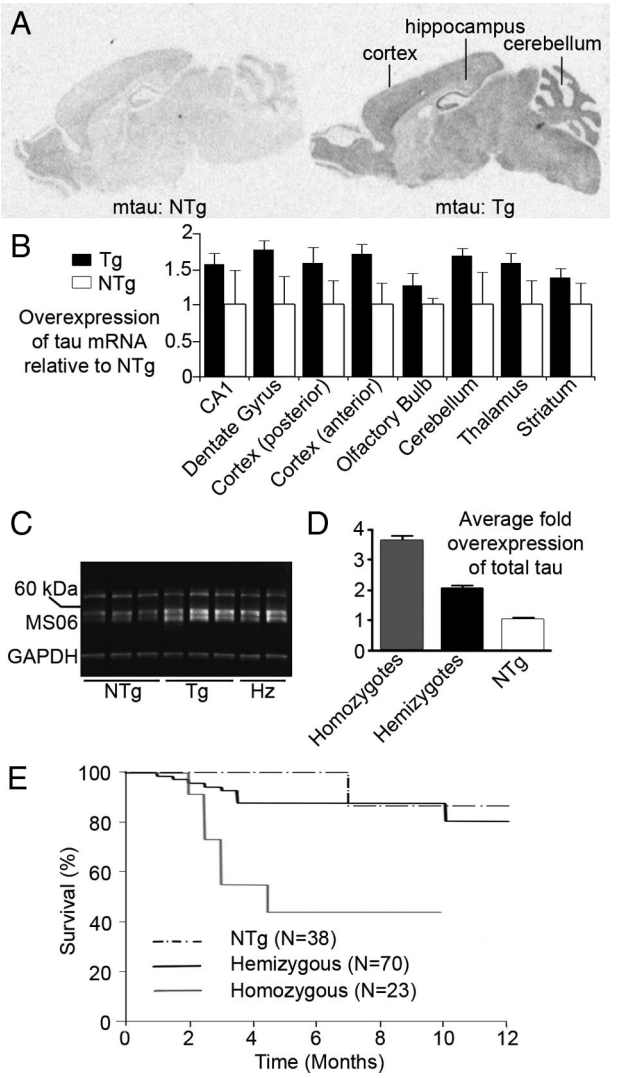

Figure 3. Expression of genomic wild-type mouse tau. **A:** *In situ* hybridization was performed on sections from 3-month-old mTau Tg and NTg mice. The mTau mice had increased mRNA expression in an identical expression pattern to NTg mice. **B:** Expression of transgenic tau mRNA ranged from 1.6 to 1.8 over the endogenous tau transcript in most brain regions including the hippocampus, cortex, and cerebellum and was similar to the results from RT-PCR analysis. **C:** Soluble tau levels in the brains of homozygous mTau mice were determined by Western analysis (MS06 antibody) at 3 months of age. Glyceraldehyde-3-phosphate dehydrogenase (GAPDH) was used as a loading control. **D:** Densitometric analysis showed that homozygous mTau mice had soluble tau levels approximately 3.5-fold over the endogenous tau level of NTg mice. Hemizygous mTau mice had soluble tau levels twofold greater than the endogenous tau level in NTg mice. **E:** Survival rate for all cohorts were calculated using Kaplan-Meier methods ($P < 0.001$ for overall log-rank test) with survival curves compared using pairwise multiple comparison procedures (Holm-Sidak method). Homozygous mTau mice had accelerated mortality (>50% death) up to 4 months of age, which was statistically significant compared with hemizygous and NTg littermates ($P = 0.025$ and $P = 0.017$, respectively).

mately 1.8-fold overexpression in hemizygotes and 3.5-fold in homozygotes (Figure 3, C and D). Although homozygotes could be generated from these lines, the resultant homozygous mice have decreased fertility consistent with our highest expressing founder animals, which were infertile with expression levels >1.8-fold. In addition, the homozygotes had increased mortality with greater than 50% of the animals dying by 4 months of age (Figure 3E). Importantly,

unlike the Htau mice, in which overexpression of the entire human tau gene, even on a mouse tau knockout background, resulted in abnormal tau exon 10 mRNA splicing ratios,[10] no aberrant splicing of mouse tau isoforms was observed in 3-month-old Tg mTau mice compared with NTg controls (data not shown), with essentially all of the tau mRNA shown to contain exon 10.

Age-Dependent Changes in Phosphorylation and Solubility in mTau Mice

Tauopathies in humans and in animal models are characterized biochemically by accumulation of insoluble hyperphosphorylated tau. This is associated with the development of pretangles and later neurofibrillary tangles that are composed of insoluble twisted filaments (PHFs) of aggregated tau of varying morphology. Western blot analysis of total lysate preparations from mTau mice, with phospho-independent (Tau5) or phospho-dependent antibodies (CP13 or PHF1), showed the presence of mouse tau migrating at 50 to 60 kDa, as well as some higher molecular weight species (64 kDa) that stained positive with the phospho-dependent antibodies. An age-related increase in total tau protein and in the hyperphosphorylated tau species, with higher apparent molecular weight, was observed with a peak at 15 months of age and then a subsequent decrease from 18 to 22 months of age, similar to the levels of 9-month-old Tg animals (Figure 4, A and B). Sarkosyl-insoluble tau migrating at 64 kDa was also detected in the mTau mice using phospho-dependent antibodies (Figure 4C). A similar insoluble tau species migrating at 64 kDa has been observed in human patients with tauopathy and has been associated with the formation of NFTs in other transgenic mouse models. Electron microscopy was performed on this sarkosyl-insoluble material and showed tau aggregates that were immunogold labeled with tau antibodies (Figure 4D).

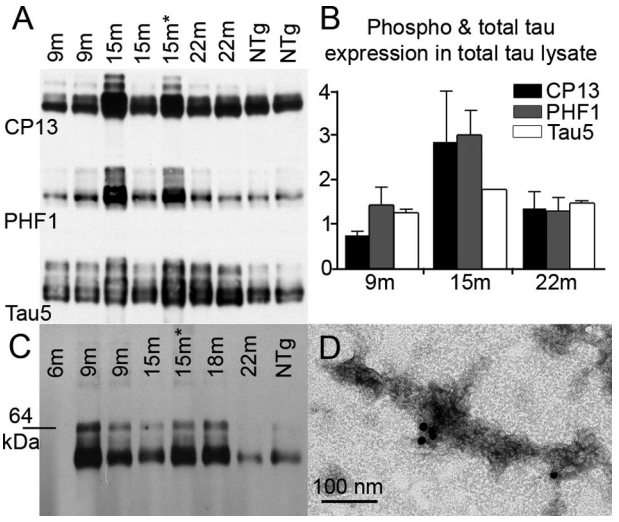

Figure 4. Soluble hyperphosphorylated tau protein increases with age, and sarkosyl-insoluble tau is present in mTau mice. **A** and **B:** Western blots and optical density analysis of total tau protein levels and phosphorylation changes with age in Tg mTau mice at various ages and NTg littermates. **Asterisk** indicates a sick animal at time of harvest. Blots were probed with phospho-tau antibody (Ab) CP13, PHF1, and total tau antibodyTau5 normalized to glyceraldehyde-3-phosphate dehydrogenase and relative to average NTgs. Statistical analysis was done by Student's *t*-test in Excel. Total tau protein expression and tau hyperphosphorylation appears to peak at 15 months of age in the mTau mice, with this age group showing a statistically significant difference between Tgs and NTgs for total tau expression (Tau5 antibody) ($P = 0.016$). This experiment was repeated five times with similar results ($n = 2$–3 per genotype per time point per gel); representative Western blots shown above. **C:** Western blot of sarkosyl-insoluble tau using PHF1 phospho-tau antibody. Western blots were repeated five times with similar results ($n = 2$–3 per genotype per time point per gel); representative Western blots shown above. **D:** Electron microscopy shows immunogold labeling, using Ab WSK44, of sarkosyl-insoluble tau aggregates in the 30 to 50% interface after sucrose gradient purification of the sarkosyl-insoluble fraction.

Age-Related Increase in Tau Pathology

The age-related biochemical changes in tau expression and hyperphosphorylation/accumulation in the mTau mice are also observed pathologically. Immunohistochemistry was performed with CP13 on brains collected from multiple male and female mTau mice between 3 and 18 months of age. Pretangle pathology (CP13-positive) was first seen as early as 6 months of age in the hemizygous mTau mice beginning in the entorhinal cortex and then spreading to other regions of the cortex and hippocampus (Figure 5). The Tau pathology increased with age, with 15- to 18-month-old mTau mice showing the most abnormal tau immunoreactivity (CP13) (Figure 5, A–H). In addition, the localization of the immunoreactivity changes with aging. In younger mice, staining of neuronal processes is observed; in contrast, by 18 months of age, the immunoreactivity is restricted to the cell bodies (Figure 5, E–H). This finding is also similar to the redistribution of tau from its normal location in the axons to the neuronal cell bodies after hyperphosphorylation in human Alzheimer's disease (AD).[23] Tau pretangle pathology also increases with gene dosage as shown by the 3-month-old homozygous mice having tau pathology similar to that of the 9-month-old hemizygous mice (Figure 5D). Immunoreactivity with other phospho-tau epitopes, PHF1 and AT8, which have been suggested to recognize later pathological changes in tau, also increase with age in the mTau mice (up to 15 to 18 months of age) (Supplemental Figure S1, see *http://ajp.amjpathol.org*). However, Gallyas silver staining was not detected, suggesting that the tau pathology formed in these mice does not progress beyond the pretangle stage. A positive correlation between age, genotype, and hyperphosphorylated tau burden in all brain regions analyzed using the Spearman rank-order correlation test, was observed with peak tau burden occurring at 15 months of age (Figure 5, I and J; Supplemental Figure 1, see *http://ajp.amjpathol.org*). Importantly, a subset (approximately 50%) of the 15-month-old cohort were characterized as moribund at the time of harvest, with weight loss, reduced grooming, urine scalding, and in 30% of this subset, an inward tail hang indicative of motor dysfunction was also observed.

Neurodegenerative Changes Accompany Pathology in mTau Mice

Other pathological analyses suggested that neurodegenerative changes are occurring in the mTau mice, includ-

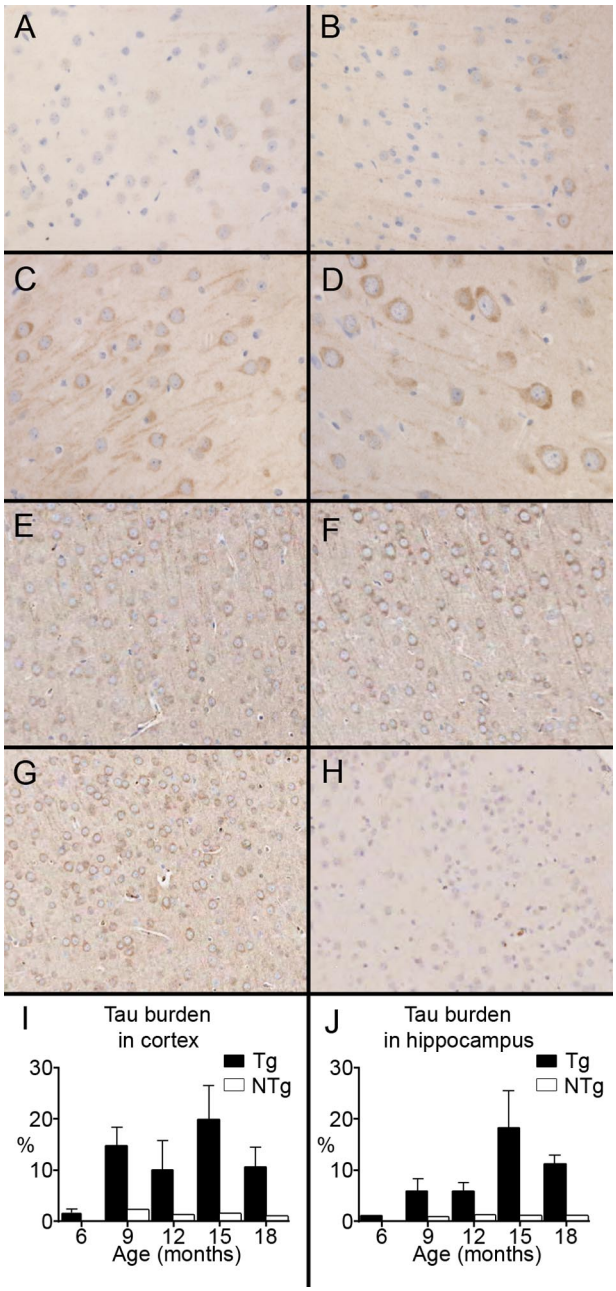

Figure 5. Tau burden increases with age and gene expression. Paraffin sections of the piriform cortex were immunostained with CP13. **A:** 3-month hemizygous. **B:** 6-month hemizygous. **C:** 9-month hemizygous. **D:** 3-month homozygous (images at ×40 magnification). **E:** 12-month hemizygous. **F:** 15-month hemizygous. **G:** 18-month hemizygous. **H:** 18-month NTg (images at ×10 magnification). Tau burden was determined using the positive pixel count algorithm of Aperio ImageScope software. Percent positivity in cortex (**I**) and hippocampus (**J**) of mTau mice is shown. Statistical analyses were performed (n = 5–9 for NTgs and 8–9 for Tgs) using the Spearman rank-order correlation test in SigmaPlot and showed positive correlations between age and tau burden in the cortex (correlation coefficient 0.263; P = 0.02) and hippocampus (correlation coefficients 0.492; P = 0.00) and between genotype and tau burden (correlation coefficient for cortex 0.548, P = 0.00; correlation coefficient for hippocampus 0.549, P = 0.00).

ing gliosis, vacuolization, and axonal degeneration. The accumulation of tau pathology in the mTau mice is accompanied by gliosis with aging (Figure 6, A–C; data not shown). In addition to the neuronal inclusions, glial tau pathology (CP13) was also observed in the mTau mice. This glial immunoreactivity appears to colocalize with oligodendrocytes but not with astrocytes or microglia (Supplemental Figure S2, see *http://ajp.amjpathol.org*; data not shown). This finding is similar to JNPL3 mice,[24] and various other models of tauopathy, which have been reported to have tau pathology in oligodendroglial cells.[25,26]

mTau mice also develop vacuolization in the neuropil occurring primarily in the hippocampus with age (Figure 6). The vacuolization tracks with transgene expression level and significantly increases with age, genotype, and tau burden (Figure 6, D–F), although the severity is variable between transgenic mice (Supplemental Figure S3, see *http://ajp.amjpathol.org*). Nontransgenic animals show either no vacuolization or little vacuolization, which does not increase with age. Electron micrographs indicate that the vacuoles in the mTau mice are derived from both degenerated axons and reactive astrocytes, possibly reflecting excitotoxic damage,[27] which has been shown to produce similar pathological changes in mice.[28] At the ultrastructural level, myelinated axons show severe vacuolization formed by splitting of the myelin lamellae at the intraperiod line. Some affected axons contained abnormal filaments that were the same size as neurofilaments, whereas other axons were completely degenerated (Figure 6, G–I).

Image analysis also showed evidence of hippocampal neuronal loss, based on quantification of neuron staining with the neuronal marker antibody NeuN, in aged (22 months) mTau mice compared with younger transgenic and age-matched NTg animals (Figure 6, J–L). Although the difference was nonsignificant, the power of the test was not the desired power for this type of study. Further analysis with a larger number and/or stereological studies will be necessary to confirm these results. These data correlates well with both the biochemical and pathological data showing an increase in tau expression and hyperphosphorylation associated with increased vacuolization derived from degenerating axons in the hippocampus up to 15 months of age, followed by a decrease in tau burden. This decrease in tau burden and hippocampal neuronal marker staining in the mTau mice may reflect neuronal loss occurring by the 22-month time point, although we cannot rule out a survivor effect based on the 50% morbundity observed in our 15-month-old cohort.

Discussion

Neurofibrillary pathology in AD and other neurodegenerative diseases results from the aggregation and deposition of hyperphosphorylated tau proteins. Unfortunately, most models overexpressing wild-type human tau isoforms,[5] including one overexpressing a genomic human tau transgene generating all six tau isoforms (8c mice),[9] have failed to produce significant NFT pathology. Interestingly, removal of the endogenous mouse tau gene in the 8c model (Htau mice) did induce age-related neuropathology[10]; although the knockout strategy used to generate this model could have unintended consequences by removal of microRNAs[29] and interactions with other

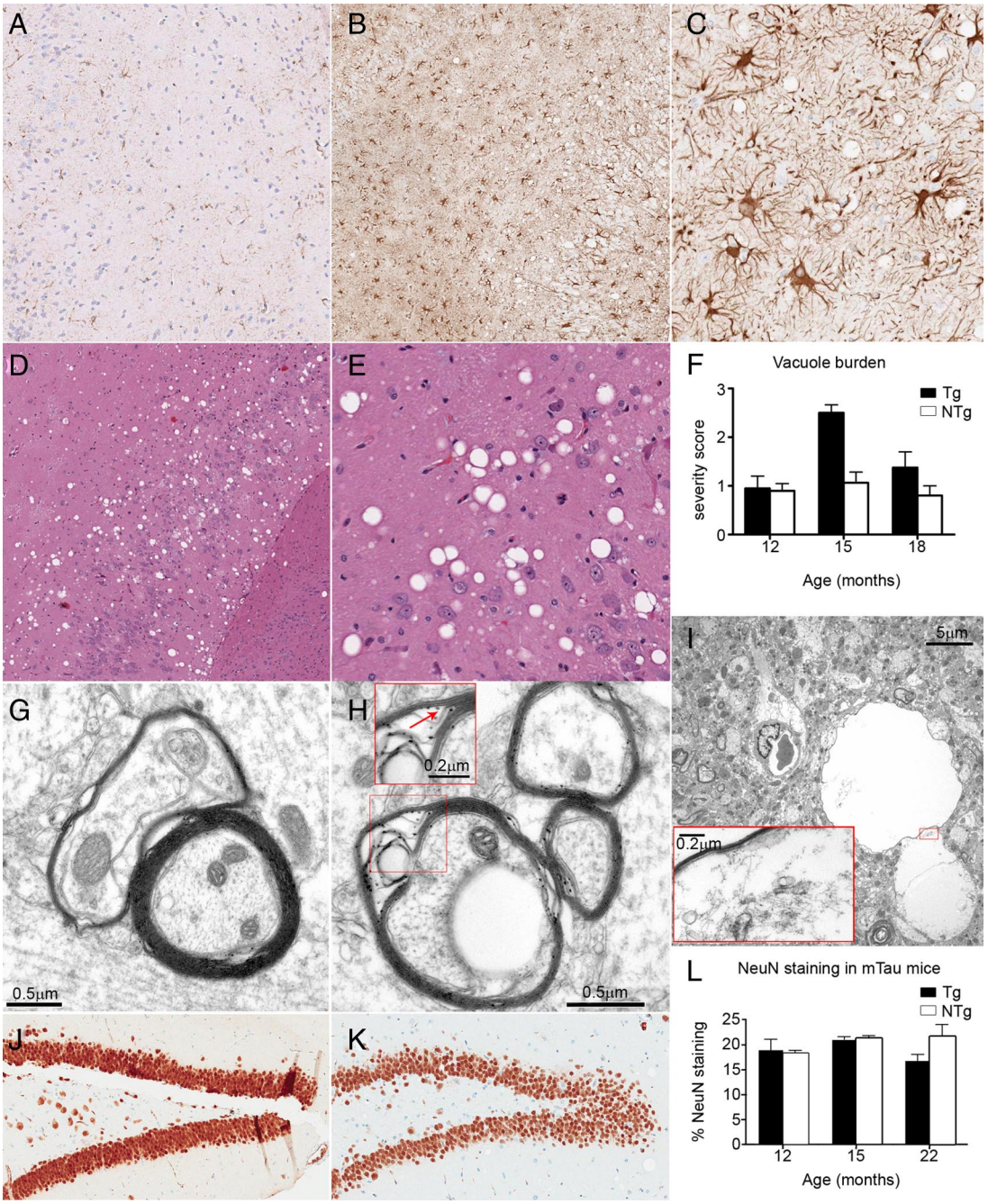

Figure 6. Neurodegenerative changes in mTau mice. **A–C:** Astrogliosis increases with age and tau gene expression in the mTau mice. Paraffin sections immunostained with GFAP show severe astrogliosis in the cortex of an 18-month Tg mTau mouse at ×5 (**B**) and ×20 (**C**) magnification. **A:** ×5 magnification of 18-month NTg for comparison. **D–F:** Vacuolization increases with age and tau burden in the mTau mice. Paraffin sections immunostained with H&E show vacuolization in the hippocampus of an 18-month Tg mTau mouse at ×5 (**D**) and ×20 (**E**) magnification. **F:** Vacuole burden in the hippocampus was determined by scoring 0 to 3 (Supplemental Figure 3, see *http://ajp.amjpathol.org*). All scoring was done blinded to genotype, age, and gender; n = 8–13 mTau mice per genotype per time point. Statistical analysis of burden scores and vacuole burden scores using the Spearman rank-order correlation test in SigmaPlot showed positive correlations between age and tau burden (correlation coefficient 0.357; P = 0.02), genotype and tau burden (correlation coefficient 0.783, P = 0.00), genotype and vacuole burden (correlation coefficient 0.325, P = 0.03), and tau burden and vacuole burden (correlation coefficient 0.316, P = 0.04). **G–I:** Electron micrographs of various stages of the vacuolization process occurring in the mTau mice. **G:** Electron micrograph showing an almost normal axon with layers of myelin tightly packed, although the innermost lamellae of the myelin sheath is starting to separate. **H:** Electron micrograph showing separation of the innermost lamellae of the myelin sheath due to axonal degeneration. Fluid infiltrates myelin sheath creating vacuolizations within an axon. **Inset:** Higher magnification image showing intramyelin vacuolization due to a split at the intraperiod line (**red arrow**) of myelin sheath of the axon. **I:** Electron micrograph showing a completely degenerated axon. **Inset:** Higher magnification image confirming that this was an axon as evidenced by the presence of the myelin sheath and filaments measuring the size of neurofilaments. **J–L:** Evidence of hippocampal neuronal loss in the mTau mice with aging. Paraffin sections of the dentate gyrus were immunostained with the neuron-specific nuclear protein, NeuN. **J:** 22-month NTg. **K:** 22-month Tg. All images are at ×10 magnification. **L:** Image analysis of NeuN staining in the hippocampus of mTau mice was performed using the positive pixel count algorithm of Aperio ImageScope software. Percent positivity in hippocampus of mTau mice is shown. Quantification of NeuN staining, which stains neurons, showed a nonsignificant trend toward neuronal loss in aged mTau mice compared with younger mTau and age-matched NTg animals. Statistical analysis was done by t-test in SigmaPlot using matched serial sections from Tg and NTg mTau mice (n = 3 to 4 NTg and 5 to 7 Tg mice per time point).

proteins. Because the primary difference between these models is the presence of the endogenous mouse tau gene, it is possible that small differences between the proteins of these two species may interfere with their ability to aggregate, thereby preventing the development of pathology. Based on this hypothesis, we have overexpressed a genomic mouse tau transgene using a BAC clone to generate a simple model of the sporadic tauopathies. As a result, regulation of the tau genomic transgene appears to mimic the endogenous gene in all aspects of regulation. In particular, exon 10 alternative splicing in the transgene-derived tau mRNA occurs in an appropriate pattern in the adult mouse brain, with >95% of the mRNA containing exon 10. The only exception is that overall levels of tau mRNA and protein are increased up to twofold in the expanded mTau lines. Higher levels of expression in some mTau founders inevitably led to reduced fertility that prevented breeding of these lines.

Controversy exists as to whether endogenous mouse tau is capable of forming aggregates or interacting with human tau, because mouse tau does not usually form aggregates *in vivo*. Mouse tau, however, has been shown to form aggregates *in vitro* that are indistinguishable from human tau aggregates.[14] Although previous studies using mutant human tau-overexpressing mice and human-specific antibodies have shown that only the human tau protein is present in the sarkosyl-insoluble fraction in these mice,[30] more recent evidence demonstrates that endogenous mouse tau can be incorporated into tangles initiated by exogenous human tau *in vivo*.[17] Our biochemical data show that overexpression of endogenous mouse tau leads to age-related hyperphosphorylation at several pathological epitopes and the accumulation of aggregated sarkosyl-insoluble tau species. Evidence from an inducible model of tauopathy in which memory loss was reversed and neuron loss ceased after tau transgene suppression despite the continued accumulation of NFTs[31,32] suggests that tau filaments in the form of NFTs are not required for tau-associated neurodegeneration but rather other earlier events, such as oligomerization may actually be primarily responsible for neurodegeneration. Thus, the mTau model may be ideally suited for studying early events linked to tau toxicity.

Hemizygous mTau mice develop pretangle pathology (CP13 positive) by 6 to 9 months of age that increases with age to include staining with other pathological phospho-epitopes such as AT8 and PHF1. However, at the tau overexpression levels achieved in the expanded lines (1.8- fold in hemizygotes), mature, Gallyas-positive NFTs were not observed, which means that this model does not yet provide a clear demonstration that mouse tau is capable of forming these late stage lesions. Homozygous mice and founders with greater than twofold overexpression levels were either infertile or had impaired breeding; thus, high levels of tau expressed from the correct promoter appear to be linked to infertility in the mTau mice. This result is interesting, given the observation that a human tau haplotype (*H2*) linked to low tau expression levels[33] is also associated with *increased fertility* in the Icelandic population.[34] Furthermore, accelerated mortality observed in the mTau lines with greater than twofold overexpression levels indicated that even moderate tau overexpression subject to regulation similar to the endogenous gene is toxic.

Early progression of tau pathology in the mTau mice occurred in brain regions, such as the entorhinal cortex, that also seem to be most vulnerable to neurofibrillary tangle formation in humans with Alzheimer's disease.[35] The abnormal tau pathology in the mTau mice increases with aging and results in a redistribution of tau from its normal location in the axons to the neuronal cell bodies after hyperphosphorylation as in AD.[23] Based on biochemical and pathological data, abnormal hyperphosphorylated tau accumulation appears to peak at 15 months of age in the mTau mice followed by a decrease at 18 to 22 months of age similar to the levels of 9-month-old Tg animals. This is accompanied by increased gliosis and vacuolization occurring primarily in the hippocampus. Tau burden positively correlates with vacuolization in the mTau mice. Electron micrographs indicate that these vacuoles, which also appear to peak at 15 months of age followed by a decrease at subsequent time points, are derived from degenerated axons.

One possible explanation for the apparent loss of tau staining after 15 months of age is neuronal degeneration and loss, as data obtained from neuron quantification showed a nonsignificant trend toward neuronal loss in aged mTau mice compared with that in younger mTau and age-matched NTg animals. This finding is consistent with other evidence for neurodegeneration, such as the increased gliosis and vacuolization resulting from degenerating axons present in the mTau mice. The findings presented here are therefore in agreement with the hypothesis that abnormal tau accumulation in upstream neurons causes a dying back process,[24] resulting in degenerating axons, vacuolization, and potentially neuronal cell body loss in the mTau model beginning around 15 months of age. Further studies are needed to determine the effects of overexpression of endogenous tau on axonal transport and synaptic function in the mTau model. Although one recent study suggested that the N terminus, which differs between mouse and human tau (only 57% homology for amino acids in the first coding exon), inhibits kinesin-dependent axonal transport,[36] it will be interesting to determine whether modest overexpression of the endogenous protein is sufficient to impair axonal transport in these animals.

The mTau model is currently unique among transgenic mouse models of tauopathy in terms of its transgene regulation, which matches that of the endogenous gene in all aspects, specifically expression pattern and alternative splicing. Also unique is the development of abnormal tau and other pathological changes including neurodegeneration with only modest overexpression of wild-type tau proteins. In this regard, the mTau line essentially models the impact of the human *H1/H1 MAPT* genotype, which has been shown to increase the level of tau expression, compared with that of other genotypes, and which increases the risk for the development of various tauopathies including progressive supranuclear palsy and corticobasal degeneration.[37–41] Another benefit of the mTau model is the overexpression of wild-type

4R tau from a genomic transgene, because adult rodents almost exclusively express the 4R tau isoform,[11] which no other line has achieved. This benefit is significant because increasing evidence points to the 4R tau isoforms being required for the development of many of the human tauopathies; however, previous transgenic mice expressing human genomic tau transgenes primarily generate 3R tau, because of a shift in the alternative splicing of the human exon 10. It will also be interesting to use the mTau model to examine the difference in exon 10 alternative splicing regulation between the human and mouse *MAPT* genes.

The importance of this model system is further underlined by recent data demonstrating that lowering endogenous tau levels in an APP transgenic mouse model results in a reduction in the Aβ-induced AD-like phenotype, specifically memory loss and excitotoxicity.[42] The mTau mice are particularly relevant for investigating the interaction between Aβ and tau during the development of Alzheimer's disease, for which reproducing this interaction using *in vivo* models has been difficult. Observing the effects of many phenotypic modifying factors in the mutant models of tauopathy and their crosses with human APP models has proven to be problematic, most likely because the rate of pathogenesis in these models is too aggressive to be readily altered. The mTau model may resolve many of these concerns, and as a result cross-breeding studies are currently underway with the intention of recapitulating key additional features of human Alzheimer's disease. Regardless of the outcome of these studies, the mTau model provides a useful tool for studying the development of nonmutant tau pathology more similar to that seen in AD and other sporadic tauopathies and a more appropriate model for the analysis of potential therapies.

Acknowledgments

We thank Dr. Peter Davies for the antibodies PHF1 and CP13; Dr. Shu-Hui Yen for the WSK44 antibody; Dr. M. Said Ghandour for the CAII antibody; Dr. Akihiko Takashima for the MS06 antibody; Linda Rousseau and Virginia Phillips for tissue sectioning; Monica Castanedes-Casey for immunostaining; Faith Conkle, Deborah Maloy, Amanda Singley, and Ed Kirkham for mouse maintenance; and Dr. Jada Lewis for helpful discussions and critical reading of this article.

References

1. Goedert M, Spillantini MG, Jakes R, Rutherford D, Crowther RA: Multiple isoforms of human microtubule-associated protein tau: sequences and localization in neurofibrillary tangles of Alzheimer's disease. Neuron 1989, 3:519–526
2. Andreadis A, Brown WM, Kosi KS: Structure and novel exons of the human tau gene. Biochemistry 1992, 31:10626–10633
3. Hutton M, Lendon CL, Rizzu P, Baker M, Froelich S, Houlden H, Pickering-Brown S, Chakraverty S, Isaacs A, Grover A, Hackett J, Adamson J, Lincoln S, Dickson D, Davies P, Pertersen RC, Stevens M, de Graaff E, Wauters E, van Baren J, Hillebrand M, Joosse M, Kwon JM, Nowotny P, Che LK, Norton J, Morris JC, Reed LA, Trojanowski J, Basun H, Lannfelt L, Neystat M, Fahn S, Dark F, Tannenberg T, Dodd PR, Hayward N, Kwok JB, Schofield PR, Andreadis A, Snowden J, Craufurd D, Neary D, Owen F, Oostra BA, Hardy J, Goate A, van Swieten J, Mann D, Lynch T, Heutink P: Association of missense and 5′-splice-site mutations in tau with the inherited dementia FTDP-17. Nature 1998, 393:702–705
4. Poorkaj P, Bird TD, Wijsman E, Nemens E, Garruto RM, Anderson L, Andreadis A, Wiederholt WC, Raskind M, Schellenberg GD: is a candidate gene for chromosome 17 frontotemporal dementia. Ann Neurol 1998, 43:815–825
5. Eriksen JL, Zehr C, Lewis J: Biologic models of neurodegenerative disorders. Edited by Duyckaerts C, Litvan I. New York, Elsevier, 2008, pp. 173–188
6. Hasegawa M, Smith MJ, Goedert M: proteins with FTDP-17 mutations have a reduced ability to promote microtubule assembly. FEBS Lett 1998, 437:207–210
7. Hong M, Zukareva V, Vogelsberg-Ragaglia V, Wszolek Z, Reed L, Miller BI, Geschwind DH, Bird TD, McKeel D, Goate A, Morris JC, Wilhelmsen KC, Schellenberg GD, Trojanowski JQ, Lee VM: Mutation-specific functional impairments in distinct tau isoforms of hereditary FTDP-17. Science 1998, 282:1914–1917
8. Dayanandan R, Van Slegtenhorst M, Mack TG, Ko L, Yen SH, Leroy K, Brion JP, Anderton BH, Hutton M, Lovestone S: Mutations in tau reduce its microtubule binding properties in intact cells and affect its phosphorylation. FEBS Lett 1999, 446:228–232
9. Duff K, Knight H, Refolo LM, Sanders S, Yu X, Picciano M, Malester B, Hutton M, Adamson J, Goedert M, Burki K, Davies P: Characterization of pathology in transgenic mice over-expressing human genomic and cDNA tau transgenes. Neurobiol Dis 2000, 7:87–98
10. Andorfer C, Kress Y, Espinoza M, de Silva R, Tucker KL, Barde YA, Duff K, Davies P: Hyperphosphorylation and aggregation of tau in mice expressing normal human tau isoforms. J Neurochem 2003, 86:582–590
11. Kosik KS, Orecchio LD, Bakalis S, Neve RL: Developmentally regulated expression of specific tau sequences. Neuron 1989, 2:1389–1397
12. Gao QS, Memmott J, Lafyatis R, Stamm S, Screaton G, Andreadis A: Complex regulation of tau exon 10: whose missplicing causes frontotemporal dementia. J Neurochem 2000, 74:490–500
13. Chohan MO, Haque N, Alonso A, El-Akkad E, Iqbal-Grundke I, Grover A, Iqbal K: Hyperphosphorylation-induced self assembly of murine tau: a comparison with human tau. J Neural Transm 2005, 112:1035–1047
14. Kampers T, Pangalos M, Geerts H, Wiech H, Mandelkow E: Assembly of paired helical filaments from mouse tau: implications for the neurofibrillary pathology in transgenic mouse models for Alzheimer's disease. FEBS Lett 1999, 451:39–44
15. Caughey B: Interactions between prion protein isoforms: the kiss of death? Trends Biochem Sci 2001, 26:235–242
16. Hasegawa K, Yamaguchi I, Omata S, Gejyo F, Naiki H: Interaction between Aβ (1-42) and Aβ (1-40) in Alzheimer's β-amyloid fibril formation in vitro. Biochemistry 1999, 38:15514–15521
17. Mocanu MM, Nissen A, Eckermann K, Khlistunova I, Biernat J, Drexler D, Petrova O, Schonig K, Bujard H, Mandelkow E, Zhou L, Rune G, Mandelkow EM: The potential for B-structure in the repeat domain of tau protein determines aggregation, synaptic decay, neuronal loss, and coassembly with endogenous tau in inducible mouse models of tauopathy. Neurobiol Dis 2008, 28:737–7448
18. Greenberg SG, Davies P: A preparation of Alzheimer paired helical filaments that displays distinct tau proteins by polyacrylamide gel electrophoresis. Proc Natl Acad Sci USA 1990;87:5827–5831
19. Abramoff MD, Magelhaes PJ, Ram SJ: Image processing with Image J. Biophoton Int 2004, 11:36–42
20. Ghandour MS, Langley OK, Vincendon G, Gombos G, Filippi D, Limozin N, Dalmasso D, Laurent G: Immunochemical and immunohistochemical study of carbonic anhydrase II in adult rat cerebellum: a marker for oligodendrocytes. Neuroscience 1980, 5:559–571
21. Iqbal K, Braak E, Braak H, Azidi T, Grundke-Iqbal I: A silver impregnation method for labeling both Alzheimer paired helical filaments and their polypeptides separated by sodium dodecyl sulfate-polyacrylamide gel electrophoresis. Neurobiol Aging 1991, 12:357–361
22. DeTure M, Ko LW, Easson C, Yen SH: assembly in inducible transfectants expressing wild-type or FTDP-17 tau. Am J Pathol 2002, 161:1711–1722
23. Mukaetova-Ladinska EB, Harrington CR, Roth M, Wischik CM: Bio-

chemical and anatomical redistribution of tau protein in Alzheimer's disease. Am J Pathol 1993, 143:565–578
24. Lin WL, Zehr C, Lewis J, Hutton M, Yen SH, Dickson DW: Progressive white matter pathology in the spinal cord of transgenic mice expressing mutant (P301L) human tau. J Neurocytol 2005, 34:397–410
25. Götz J, Tolnay M, Barmettler R, Chen F, Probst A, Nitsch RM: Oligodendroglial tau filament formation in transgenic mice expressing G272V tau. Eur J Neurosci 2001, 13:2131–2140
26. Higuchi M, Zhang B, Forman MS, Yoshiyama Y, Trojanowsk JQ, Lee VM: Axonal degeneration induced by targeted expression of mutant human tau in oligodendrocytes of transgenic mice that model glial tauopathies. J Neurosci 2005, 25:9434–9443
27. Scallet AC, Ye X: Excitotoxic mechanisms of neurodegeneration in transmissible spongiform encephalopathies. Ann NY Acad Sci 1997, 825:194–205
28. Olney JW, Wozniak DF, Farber NB: Excitotoxic neurodegeneration in Alzheimer disease: new hypothesis and new therapeutic strategies. Arch Neurol 1997, 54:1234–1240
29. Osokine I, Hsu R, Loeb GB, McManus MT: Unintentional miRNA ablation is a risk factor in gene knockout studies: a short report. PLoS Genet 2008, 4:1–3
30. Sahara N, Lewis J, DeTure M, McGowan E, Dickson DW, Hutton M, Yen SH: Assembly of tau in transgenic animals expressing P301L tau: alteration of phosphorylation and solubility. J Neurochem 2002, 83:1498–1508
31. Santacruz K, Lewis J, Spires T, Paulson J, Kotilinek L, Ingelsson M, Guimaraes A, DeTure M, Ransden M, McGowan E, Forster C, Yue M, Orne J, Janus C, Mariash A, Kuskowski M, Byman B, Hutton M, Ashe KH: suppression in a neurodegenerative mouse model improves memory function. Science 2005, 309:476–481
32. Ramsden M, Kotilinek L, Forster C, Paulson J, McGowan E, Santacruz K, Guimaraes A, Yue M, Lewis J, Carlson GA, Hutton M, Ashe KH: Age-dependent neurofibrillary tangle formation, neuron loss, and memory impairment in a mouse model of human tauopathy (P301L). J Neurosci 2008, 25:10637–10647
33. Pittman AM, Meyers AJ, Abou-Sleiman P, Fung HC, Kaleem M, Marlowe L, Duckworth J, Leung D, Williams DS, Kilford L, Thomas N, Morris CM, Dickson D, Wood NW, Hardy J, Lees AJ, de Silva R: Linkage disequilibrium fine mapping and haplotype association analysis of the tau gene in progressive supranuclear palsy and corticobasal degeneration. J Med Genet 2005, 42:837–846
34. Stefansson H, Helgason A, Thorleifsson G, Steinthorsdottir V, Masson G, Barnard J, Baker A, Jonasdottir A, Ingason A, Gudnadottir VG, Desnica N, Hicks A, Gylfason A, Gudbjartsson DF, Jonsdottir GM, Sainz J, Angnarsson K, Birdgisdottir B, Ghosh S, Olafsdottir A, Cazier JB, Kristjansson D, Frigge ML, Thorgeirsson TE, Gulcher JR, Kong A, Stefansson K: A common inversion under selection in Europeans. Nat Genet 2005, 37:129–137
35. Braak H, Braak E: Neuropathological stageing of Alzheimer-related changes. Acta Neuropathol 1991, 82:239–259
36. LaPointe NE, Morfini G, Pigino G, Gaisina IN, Kozikowski AP, Binder LI, Brady ST: The amino terminus of tau inhibits kinesin-dependent axonal transport: implications for filament toxicity. J Neurosci Res 2009, 87:440–451
37. Kwok JB, Teber ET, Loy C, Hallupp M, Nicholson G, Mellick GD, Buchanan DD, Silburn PA, Schofield PR: haplotypes regulate transcription and are associated with Parkinson's disease. Ann Neurol 2004, 55:329–334
38. Houlden H, Baker M, Morris HR, MacDonald N, Pickering-Brown S, Adamson J, Lees AJ, Rossor MN, Quinn NP, Kertesz A, Khan MN, Hardy J, Lantos PL, St. George-Hyslop P, Munoz DG, Mann DMA, Lang AE, Bergeron C, Bigio EH, Litvan I, Bhatia KP, Dickson D, Wood NW, Hutton M: Corticobasal degeneration and progressive supranuclear palsy share a common tau haplotype. Neurology 2001, 56:1702–1706
39. Di Maria E, Tabaton M, Vigo T, Abbruzzese G, Bellone E, Donati C, Frasson E, Marchese R, Montagna P, Munoz DG, Pramstaller PP, Zanusso G, Ajmar F, Mandich P: Corticobasal degeneration shares a common genetic background with progressive supranuclear palsy. Ann Neurol 2000, 47:374–377
40. Conrad C, Andreadis A, Trojanowsk JQ, Dickson D, Kang D, Chen X, Wiederholt WC, Hansen L, Masliah E, Thal U, Katzman R, Xia Y, Saitoh T: Genetic evidence for the involvement of tau in progressive supranuclear palsy. Ann Neurol 1997, 41:277–281
41. Baker M, Litvan I, Houlden H, Adamson J, Dickson D, Perez-Tur J, Hardy J, Lynch T, Bigio EH, Hutton M: Association of an extended haplotype in the tau gene with progressive supranuclear palsy. Hum Mol Genet 1999, 8:711–715
42. Roberson ED, Scearce-Levie K, Palop JJ, Yan F, Cheng IH, Wu T, Gerstein H, Yu GQ, Mucke L: Reducing endogenous tau ameliorates amyloid β-induced deficits in an Alzheimer's disease mouse model. Science 2007, 316:750–754